Experimental findings concerning the evolution of breach resulting from the seepage at earthen dams under different scenarios

Mehmet Şükrü Güney[1*], and *Ruti* Politi[1]

[1]Izmir University of Economics, Faculty of Engineering, Department of Civil Engineering, İzmir, Türkiye,

Abstract. Piping is one of the major phenomena which threaten earth-fill dam stability and safety. Piping depends on several geometric, hydraulic and geotechnical parameters and can cause erosion within the dam structure. This study involves time-dependent evolutions of the breach shape and flow rate from the breach corresponding to four different scenarios. Both homogeneous and clay cored earth-fill dams were constructed by using a sand-clay mixture consisting of 85% sand and 15% clay. The weak layer was created at bottom or at top of the dam bodies. The temporal evolution of the breaches was recorded using high-quality cameras installed at upstream, downstream and lateral sides of the flume. A magnetic flow meter placed on the discharge pipe measured the inflows. The flow rates from the breach were calculated by using the continuity equation describing the mass conservation. The so-obtained experimental findings are presented and interpreted. The primary objective of these experimental studies is to enable the calibration and validation of the numerical models employed in the corresponding computational analyses. This study revealed that in the laboratory conditions, it is also possible to monitor the evolution of breach geometries resulting from piping by using rock salt or by creating a weak non-compacted layer. As expected, the internal erosion began at downstream side and progressed toward upstream. Numerical analysis corresponding to the second scenario has been achieved and an acceptable compatibility between experimental and numerical results was found.

1 Introduction

Piping is one of the major phenomena which threaten earth-fill dam stability and safety. Piping depends on several geometric, hydraulic and geotechnical parameters and can cause erosion within the dam structure.

This paper presents experimental findings on the progression of dam failure by seepage under four scenarios, in which the dam bodies are constructed from a sand-clay mixture with a grain size of D_{50} = 0.30 mm. The objective of this research is to compare the experimental findings corresponding to two homogenous dams and two clay cored earth-fill dams to

* Corresponding author: sukru.guney@ieu.edu.tr

© The Authors, published by EDP Sciences. This is an open access article distributed under the terms of the Creative Commons Attribution License 4.0 (https://creativecommons.org/licenses/by/4.0/).

contribute to the understanding of the breach mechanism and to obtain measured data for the researchers who deal with numerical analyses related to piping in earth-fill dams.

2 Experimental Procedure

The experiments were performed in the rectangular flume shown in Fig.1. The dimensions of the flume were 1.00 m (width), 0.81 m (height), and 5.44 m (length). The bottom of the flume consisted of sheet metal whereas its sides were made of tempered glass for the better observation of the temporal breach areas obtained from the cameras records. The lower channel served as water supplying and soil collecting container. The dam bodies were constructed at the upper channel. The dams were designed and constructed with side slopes of 1V:1.5H. A pump whose flow rate was measured by means of a flowmeter placed at its downstream, provided water circulation in the closed system.

The dam bodies were constructed using a sand-clay mixture composed of 85% sand and 15% clay. The sands used in the mixture were quartz bought from a commercial company. The clay used in the mixture and in the core consisted of kaolin furnished by a company which manufactures different construction materials. Before the piping experiments, some known soil mechanics experiments such as sieve and hydrometer analyses, consolidation test, permeability test, direct shear test and proctor tests were realised.

The particle size distribution curve of the mixture is given in Fig. 2a. According to Unified Soil Classification System, the mixture was identified as Clayey Sand with symbol SC. The specific gravity of the mixture was determined as 2.63. The permeability of the mixture was calculated as $k=4.66 \times 10^{-4}$ cm/s. The cohesion and internal friction values obtained from the direct shear test, were found as 15.33 kPa and 33.93º, respectively. Proctor test results were depicted in Fig. 2b. The details concerning soil mechanics tests results and the piping experiments findings mentioned in this paper are given in the papers presented in the scientific meetings held in the past, such as [1] and [2].

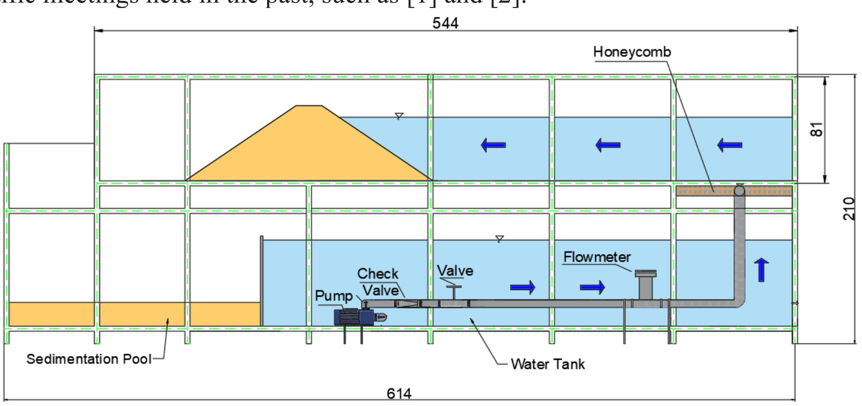

Fig. 1. Experimental set-up (all dimensions are in cm.)

The number of proctor test blows was selected as 13 instead of 25 to promote piping within the dam body. When the dam bodies were constructed, each layer was prepared so that the bulk density of 2 g/cm^3 was satisfied. Each layer of 14 cm initial thickness was reduced to 10 cm after the compaction.

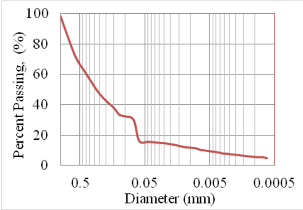

(a)

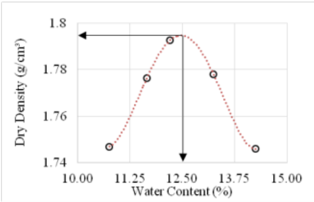

(b)

Fig. 2. a) Grain size distribution and b) dry density-water content relationship.

Some construction stages of the dam body are illustrated in Fig. 3. The mixture was carefully placed and subsequently compacted with the help of a plate and proctor hammer. L-shaped moulds were used during the construction of each layer. Following the construction of the dam body, the moulds were removed and any excess soil was trimmed by using a trowel.


(a) (b) (c) (d)

Fig. 3. Some stages of the dams construction: a) Spreading out of the mixture, b) Creating weak layer, c) Compacting, d) After compaction

The details regarding the dam dimension and weak layer are presented in Table 1. The first two scenarios correspond to the homogeneous dams while the 3rd and 4th scenarios are related to the earthen dams with clay core.

The cameras were placed at flume ends and lateral sides to monitor the experiments and record the temporal evolutions of the breaches. An electromagnetic sensor was installed on the flume wall to adjust the water depth in the upper channel so that the pump starts and stops at predetermined water levels. The pump restarted when the water level in the upper channel (reservoir) decreased by 10% of its initial value.

Table 1. Dam geometry and weak layer characteristics.

Scenario Number	**1**	**2**	**3**	**4**
Height (m)	0.6	0.6	0.65	0.65
Bottom width (m)	2	2	2	2
Crest width (m)	0.20	0.20	0.05	0.05
Weak layer type	Rock salt	Hole	Rock salt	Non-compacted soil
Weak layer location	Bottom	Top	Bottom	Top
Weak layer cross-section shape	Square	Circular	Square	Square
Weak layer dimensions	5 x 5 cm^2	2 cm diameter	5 x 5 cm^2	5 x 5 cm^2

3 Experimental Findings

Some pictures obtained from the camera records are given below. In the case of the homogenous dam at which the weak layer was located at bottom (Scenario 1), the time t=0 corresponds to the time at which the breach appeared at upstream face. In the other three scenarios, t = 0 corresponds to the time just after the seepage starts on the considered face.

Fig. 4 to Fig. 11 illustrate some pictures obtained from camera records.

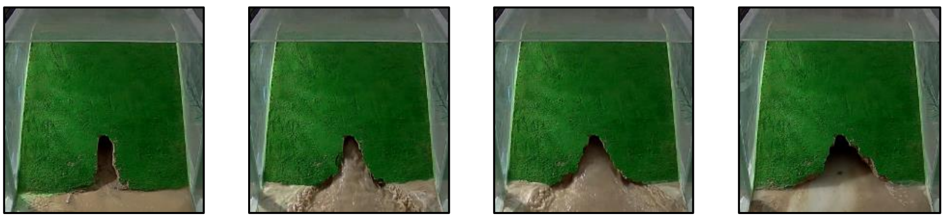

(a) (b) (c) (d)

Fig. 4. Some pictures obtained from the camera placed at downstream corresponding to the 1st scenario a) t = 0 s, b) t = 20 s c) t = 30 s, d) t = 315 s.

(a) (b) (c) (d)

Fig. 5. Some pictures obtained from the camera placed at downstream corresponding to the 2nd scenario a) t = 0 s, b) t = 140 s, c) t = 420 s, d) t = 780 s.

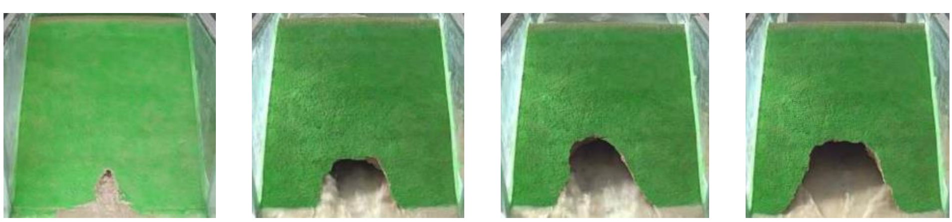

(a) (b) (c) (d)

Fig. 6. Some pictures obtained from the camera placed at downstream corresponding to the 3rd scenario a) t = 0 s, b) t = 185 s c) t = 245 s, d) t = 360 s.

(a) (b) (c) (d)

Fig. 7. Some pictures obtained from the camera placed at downstream corresponding to the 4th scenario a) t = 0 s, b) t = 515 s, c) t = 2230 s, d) t = 2575 s.

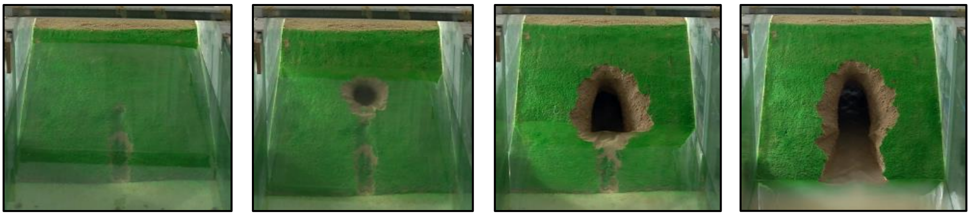

(a) (b) (c) (d)

Fig. 8. Some pictures obtained from the camera placed at upstream corresponding to the 1st scenario a) t = 0 s, b) t = 15 s, c) t = 50 s, d) t = 310 s.

(a) (b) (c) (d)

Fig. 9. Some pictures obtained from the camera placed at upstream corresponding to the 2nd scenario a) t = 0 s, b) t = 140 s, c) t = 420 s, d) t = 780 s.

(a) (b) (c) (d)

Fig. 10. Some pictures obtained from the camera placed at upstream corresponding to the 3rd scenario a) t = 0 s, b) t = 185 s, c) t = 240 s, d) t = 360 s.

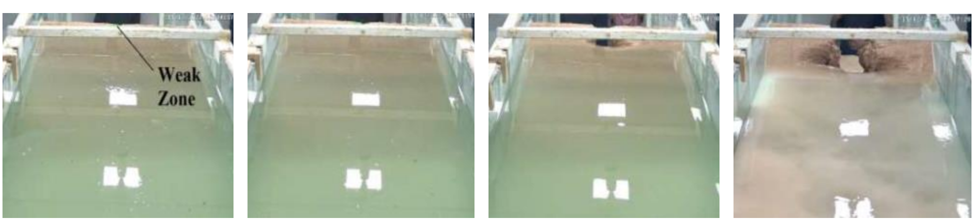

(a) (b) (c) (d)

Fig. 11. Some pictures obtained from the camera placed at upstream corresponding to the 4th scenario a) t = 0 s, b) t = 515 s, c) t = 2230 s, d) t = 2400 s.

The water depth values in the reservoir were obtained by using the related camera records. The breach geometry and its shape variation were evaluated from the examination of the images recorded by both cameras located at upstream and downstream parts.

Get-data Graph Digitizer 2.26 software was used to determine the coordinates of the breach boundaries.

The Gauss Area formula was used to calculate the time-dependent breach areas.

The outflow discharges from the breach were determined by using the common mass conservation principle (continuity equation); the difference between the average inflow and

https://doi.org/10.1051/e3sconf/202672506003

outflow rates during a specified time interval was equated to the rate of change in reservoir water volume over time:

$$\Delta S = \left(Q_{pump} - Q_{breach}\right) \cdot \Delta t \qquad (1)$$

where Q_{pump} is the pump flow rate, Q_{breach} is the discharge of water outgoing from the breach, and ΔS is the change in reservoir water volume during the time interval Δt.

The temporal water depths in the channel for the 1st and 2nd scenarios are given in Fig. 12a. The water depth variations over time for the earthen clay-cored dams are presented in Fig. 12b.

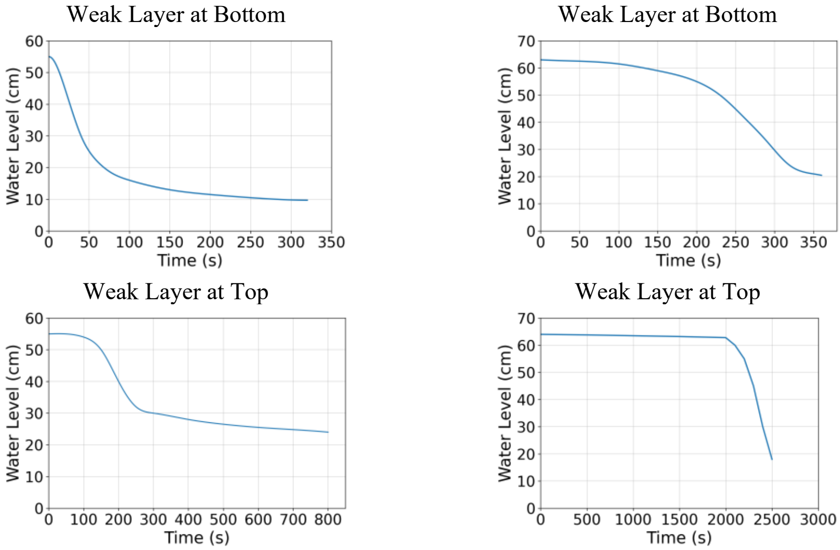

(a) (b)

Fig. 12. Temporal water depths in a) homogeneous dams b) clay-cored dams

The second scenario was repeated by applying spray paint to the dam body in order to monitor the erosion process by using the image processing technique for the breach surface areas and compare them to those obtained from the Gauss area formula [3]. The camera records corresponding to temporal development of the breach at downstream and upstream faces are given in Fig. 13 and Fig. 14 respectively.

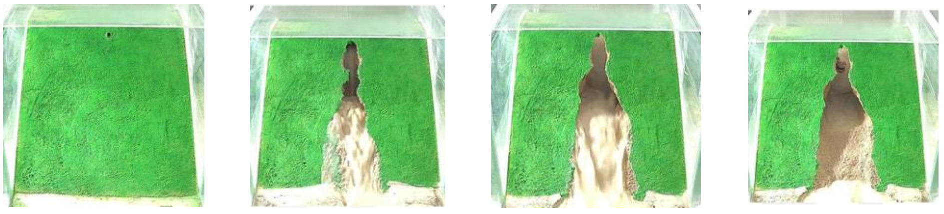

(a) (b) (c) (d)

Fig. 13. Some pictures obtained from the camera placed at downstream corresponding to the repeated experiment case a) t = 0 s, b) t = 180 s, c) t = 380 s, d) t = 570 s.

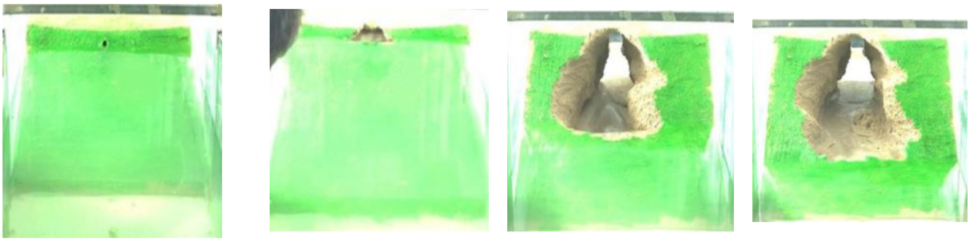

(a) (b) (c) (d)

Fig. 14. Some pictures obtained from the camera placed at upstream corresponding to the repeated experiment case a) t = 0 s, b) t = 180 s, c) t = 380 s, d) t = 570 s.

The comparison of these figures with Fig. 5 and Fig. 9 revealed the similarity of the breach development patterns in both experiments, thus demonstrating also the repeatability of the performed experiments.

4 Results and Discussion

The temporal discharges outgoing from the breach for different scenarios are given in Fig. 15.

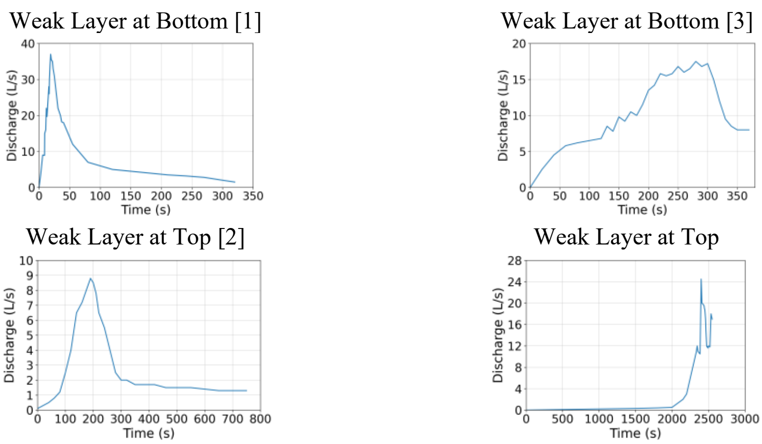

(a) (b)

Fig. 15. Temporal breach discharges in a) homogeneous dams b) clay-cored dams.

The time-dependent variations of the breach areas at downstream and upstream faces of the homogeneous dams are shown in Fig. 16a and Fig. 16b, respectively.

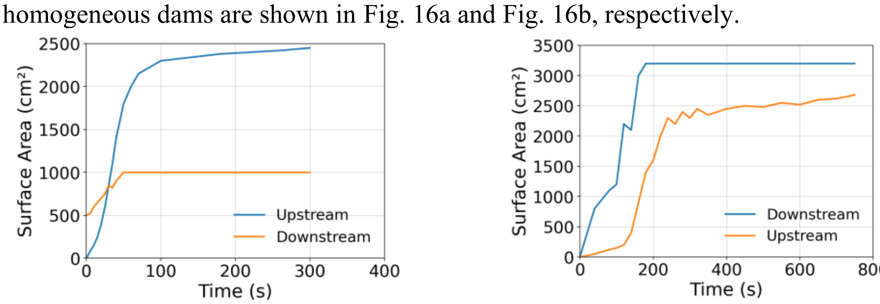

(a) (b)

Fig. 16. Temporal variations of the total breach area at downstream and upstream in the case of homogeneous dams a) Scenario 1, and b) Scenario 2.

The time-dependent evolution of the breach areas at downstream and upstream faces of the clay-cored earthen dams are shown Fig. 17a and Fig. 17b, respectively.

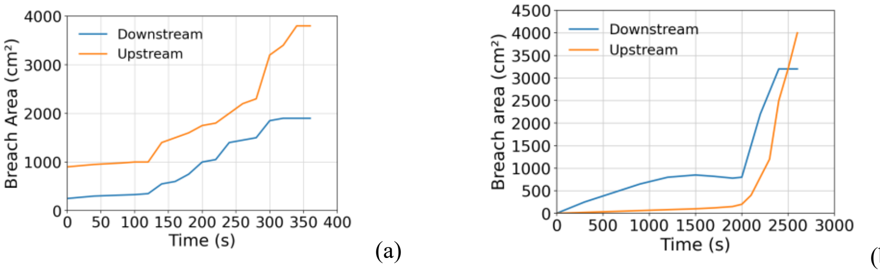

Fig. 17. Temporal variations of the total breach area at downstream and upstream in the case of clay-cored earthen dams a) Scenario 3, and b) Scenario 4.

The results of the comparative experiments are provided in Table 2.

Table 2. Comparative analysis of experimental findings across scenarios.

Scenario Number	1	2	3	4
Max. flow rate Q_{max} (L/s)	37.40	8.62	17.65	24.90
Max. breach area at downstream B_{dmax} (cm^2)	996	3247	1911	3219
Max. breach area at upstream B_{umax} (cm^2)	2499	2643	3826	4003

This study was realized by using the available opportunities of the project budget and its required completion time. In the scope of the project, 6 homogeneous dams and 4 earthen dams with clay core were tested. The repeatability of such experiments was also checked in the scenario corresponding to the homogeneous dam with seepage starting at its middle part. The compatibility between the results of two experiments was found to be satisfactory.

This study revealed that in the laboratory conditions, it is also possible to monitor the temporal evolution of the breaches resulting from piping by using rock salt or by creating a weak non- compacted layer.

In all scenarios, erosion initiated at the downstream side, progressed inward and propagated toward the upstream direction. When the weak layer was at top, the breach reached upstream quite quickly but it took much longer time when the weak layer was located at bottom, as expected.

The highest peak flow rate was recorded bottom seepage in the homogeneous dam (Scenario 1), because of the important water head value over the breach. This was not the case for the dam with clay core due to the important width of the clay core at lower part.

It was revealed that the breach areas were greater at upstream face, except in the 2nd scenario where the seepage was initiated by means of a circular tunnel along which free surface flow occurred. Breach areas were more significant when the weak layer was at top because of the available space for the breach development. The rigid (metallic) flume bottom prevented the breach progress.

The occurrence and temporal progression of the complex piping phenomenon are influenced by several geometric, hydraulic, and soil parameters. The variation in dam type and its geometry, water level in the reservoir, soil mixture composition and compaction amount would induce different breach development patterns. For these reasons, it would be appropriate to conduct as many experimental studies and numerical analyses as possible. Such researches will contribute new resources to the literature about piping caused by the seepage in both homogeneous and clay-core earth dams.

Numerical analysis corresponding to the second scenario has been already achieved and satisfactory agreement between experimental and numerical results was observed.

Acknowledgements

The authors thank the Scientific and Technological Research Council of Turkey (TUBITAK) for supporting financially this study through the project 119M609.

References

[1] M. S. Guney, M. Okan, E. Dumlu, A. Bor, P. Aklık, and G. Tayfur, Experimental Study of the Evolution of the Breach and the Discharge Through the Breach Resulting from Piping due to Seepage at the Earth-Fill Dam Top, presented at the 39th IAHR World Congress, Granada, Spain, (2022).

[2] M. S. Guney, E. Dumlu, M. Okan, and Y. Kalyoncu, Experimental Study of the Evolution of the Breach and the Discharge Through the Breach Resulting from Piping Due To the Seepage at the Upper Part of Earth-Fill Dam with Clay Core, presented at the Balkan 7th International Conference on Applied Sciences, Skopje, (2023).

[3] M. Ş. Güney, M. Okan, E. Dumlu, A. Bor, G. Tayfur, and P. Aklık, Experimental Study of Evolution of Breach Resulting from Piping at Upper Part of Earth-Fill Dam, Turkish Journal of Civil Engineering*,* **36**(2), 97-119, (2025).